Available online at www.sciencedirect.com
SCIENCE DIRECT®
Tetrahedron: Asymmetry
Tetrahedron: *Asymmetry* 16 (2005) 243–253

Synthesis and characterisation of hexa- and tetrasaccharide mimics from acetobromomaltotriose and acetobromomaltose, and of *C*-disaccharide mimics from acetobromoglucose, obtained by electrochemical reduction on silver

Marco Guerrini,[a] Sara Guglieri,[a] Roberto Santarsiero[a] and Elena Vismara[b,*]

[a]*Istituto di Ricerche Chimiche e Biochimiche 'G. Ronzoni', Via G. Colombo 81, I-20133 Milano, Italy*
[b]*Dipartimento di Chimica, Ing. Chimica e Materiali 'G.Natta' Politecnico, Via Mancinelli 7, I-20131 Milano, Italy*

Received 2 November 2004; accepted 19 November 2004
Available online 5 January 2005

Abstract—Glucose-based glycomimetics characterised by a direct *C*-interglycosidic bond were synthesised from acetobromomaltotriose (**ABMT**), acetobromomaltose (**ABM**) and acetobromoglucose (**ABG**). Electroreduction on silver cathode of acetobromomaltotriose afforded the diastereoisomeric hexasaccharide mimics **1**–**3**, which were deacetylated to **4**–**6**. The same procedure afforded biglucosyl derivatives **10**–**12** from acetobromoglucose and tetrasaccharide mimics **15** and **16** from acetobromomaltose. The C–Br bond was reduced affording an intermediate anomeric radical whose coupling formed the new C–C bond. The electrochemical induced coupling resulted in a one-pot reaction to double the parent sugar units. NMR and molecular modelling were used for the conformational analysis of the diastereoisomers.

1. Introduction

C-Glycosides have gained interest as molecules of potential biological activity, also useful for enzymatic and metabolic studies.[1] Some examples of mixed *O*/*C*-glycosides were also investigated.[2] We described an electrochemical approach to *C*-disaccharide like mimics, that is the reduction of glucosyl bromide[3] in acetonitrile at a silver electrode, a way already extensively applied to glycoside syntheses (Fig. 1).[4,5] Some evidence prompted us to explain these syntheses via a radical pathway, that is the dimerisation of carbon-centred radicals generated by electroreduction of C–X.[3–5] With this procedure, both flexible and rigid C–C bonds can be build between two sugar units (Fig. 1). Radical coupling is not stereoselective and generally afforded statistical mixtures of the possible diastereoisomers. Electroreduction of acetobromoglucose **ABG** afforded biglucosyl derivatives **7**–**9** (Scheme 1) that were separated by fractioned crystallisation.[3] Also tetrasaccharides **13** and **14** shown in Scheme 1 were successfully obtained from acetobromomaltose **ABM**.[4] They were isolated by flash chromatography on silica gel. The β,β isomer was not found, probably as it was dispersed in mixed fractions. In addition, **9** was the worst isomer to purify as it did not crystallise and remained in the mother liquor.

The present work was addressed to synthesise maltohexaose mimics from acetobromomaltotriose **ABMT**, with the aim of testing if the electroreduction coupling is still working to also double a trisaccharide moiety. This attempt could be meaningful not only as an extension of the electrochemical approach, but also because there have been many reports about the biological activity of oligosaccharides made by a very few numbers of sugar units. It is well-known that sialyl Lewis is a tetrasaccharide, ligand of selectins and obviously mimics of few sugar units.[6a] Furthermore, possible oligomers related to saccharide binding to animal lectins can be made from four to six units.[6b] Finally, concerning the characteristics of heparin binding, oligosaccharide size starts from four monomers[7a] and sulfated oligosaccharide-based inhibitors concerning angiogenesis and heparanase activity[7b] can be made by four to six saccharide units.

The present work was also addressed to build up a small library of di-, tetra- and hexaglucose-based

* Corresponding author. Tel.: +39 02 23993088; fax: +39 02 23993080; e-mail: elena.vismara@polimi.it

0957-4166/$ - see front matter © 2004 Elsevier Ltd. All rights reserved.
doi:10.1016/j.tetasy.2004.11.052

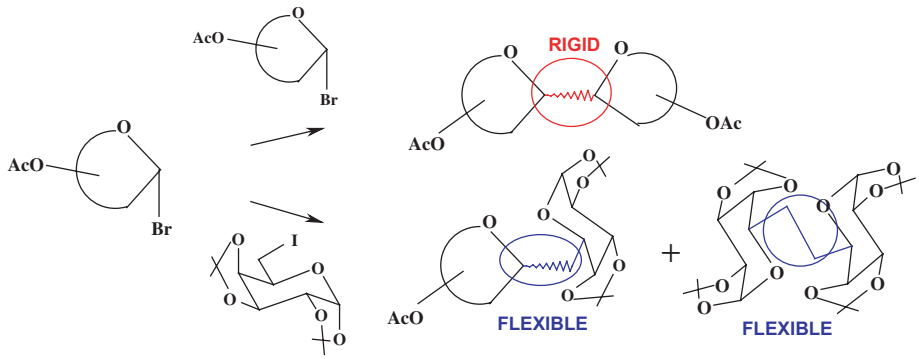

Figure 1. Products available via an electrochemical approach to *C*-disaccharide-like mimics.

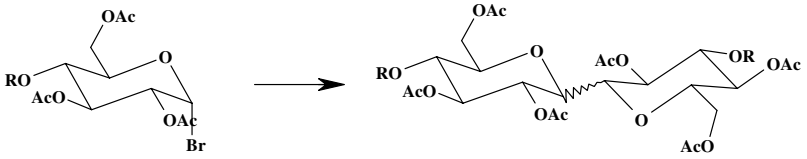

R = Ac (**ABG**) ⇒ **7** (α,α) **8** (α,β) **9** (β,β)

R = tri-Ac-4-*O*-(α-D-glucopyranosyl) (**ABM**) ⇒ **13** (α,α) **14** (α,β) not found (β,β)

Scheme 1. Diastereoisomer compounds from electroreduction of **ABG** and **ABM**.

glycomimetics characterised by a direct *C*-interglycosidic bond. This library presents different aspects of interest. Some of them are common with the chemistry of *C*-glycosides, as the proposed *C*-interglycosidic bond introduces the same factors of stability largely discussed in the literature. Indeed, as far as we know, direct *C*-interglycosidic bond has remained practically unexplored, thus the library object of this paper can make possible to study if and how a direct anomeric C–C link might affect conformational properties, resulting in new potential biological activities. In this context, molecular modelling analysis of compounds of different configurations at the new C–C bond and of different chain elongation was taken into account to compare with data obtained by NMR. Finally, the proposed library components can be used as original chiral building blocks.

2. Results and discussion

2.1. Electrochemical parameters and preparative electrolyses

Potentiostatic preparative electrolyses on silver were run based on cyclic voltammetry experiments. Voltammograms of **ABG** (Fig. 2), **ABM** and **ABMT** are quite similar and showed one irreversible peak at the redox potential E_p where C–X bond undergoes a single electron-transfer reduction (Table 1); the following elimination of the halogen anion leads to an intermediate anomeric radical that dimerises; the mechanism being illustrated with **ABG** in Scheme 2. The electrode process on the silver cathode appears complex. It favours radical dimerisation, a process that needs high radical concentration and generally does not occur in significant amount due to the high reactivity of radicals that does not allow a suitable concentration to dimerise to be reacted. We found that glycals always accomplished dimers formation during the electroreduction of **ABG**, **ABM** and **ABMT** on silver. In the single wave of the voltammograms on silver there is probably an overlapping of two peaks. The first one at a more positive potential is responsible for the dimer formations due to the passage of a single electron. The second one at more negative potential is due to the passage of two electrons, responsible of glycal formation. Glycal formation process was interpreted as a two electron C–Br bond cleavage coupled to a very fast elimination of the acetate anion, see Scheme 2 that shows the mechanism for **ABG**. The concerted elimination of the acetate anion can explain the absence of glycitol that would be formed from an anomeric intermediate carbanion. Experiments run on **ABG** under different potentiostatic conditions on silver supported the overlapping hypothesis as the ratios glucal/dimers changed with the redox potential (Fig. 3). At more positive potentials, dimers prevailed while the amount of glucal increased at more negative potentials. It seems that the formation of glycals on silver cannot be avoided and it is the more negative aspect of this approach as it decreased the dimerisation yields. The electroreduction of halosugars was studied also on glassy carbon, the so-called innocent electrode widely used to avoid any interactions between the electrode material and the substrate to be reduced. Cyclic voltammetry was run and once again showed a single irreversible peak, the redox potentials being more negative than on silver, see Table 1 and Figure 2. This phenomenon is common for a large number of halosugars and for simple alkyl halides, too.[8]

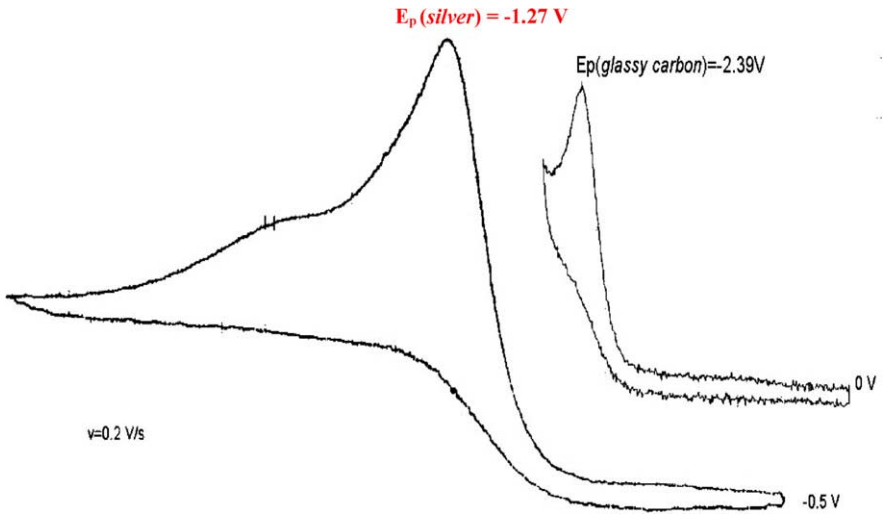

Figure 2. Cyclic voltammetry of **ABG** on silver and glassy carbon.

Table 1. Reduction peak potentials of **ABG**, **ABM** and **ABMT** on silver and on glassy carbon

	E_p (Ag)/V (vs SCE)[a]	E_p (GC)/V (vs SCE)[a]
ABG	−1.27	−2.39
ABM	−1.29	−2.43
ABMT	−1.48	Not determined

[a] SCE = saturated calomel electrode.

Concerning the halosugars of interest in this paper, **ABG** was the more investigated from a mechanistic point of view and it was submitted to potentiostatic preparative electrolysis also on graphite, giving dimerisation only as a side reaction, the main product being the triacetylglucal (Scheme 2). The single peak on GC is mainly due to a two-electron process consistent with glucal formation. It is evident that silver and GC have different behaviour towards halosugars. In the cyclic voltammetry, silver electrode is electrocatalytic with respect to glassy carbon, probably due to the well-known affinity between silver and halogen atoms. As the product distributions in preparative electrolyses also dramatically changed, the differences between silver and GC are huge. An important question is why dimers are typically formed on silver. A possible explanation could be that there is an interaction of silver with carbohydrate intermediate radicals forming a sort of metal-free radical complex of relatively longer life than simple radicals: they survive enough time to couple. On carbohydrate moiety, the high number of oxygen atoms with free doublets of electrons could interact with the electrons of the silver lattice. In 1961, Kochi and Rust observed a quite similar phenomenon, that the interaction of radicals

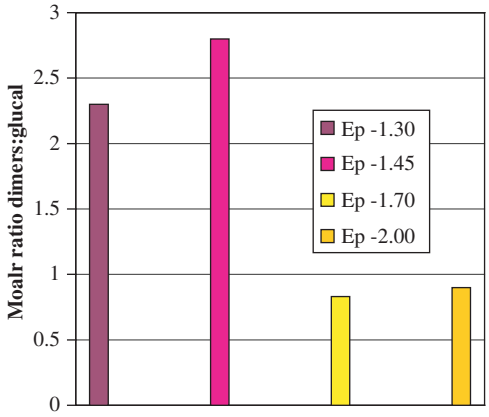

Figure 3. Reduction of **ABG** on silver at different E_p.

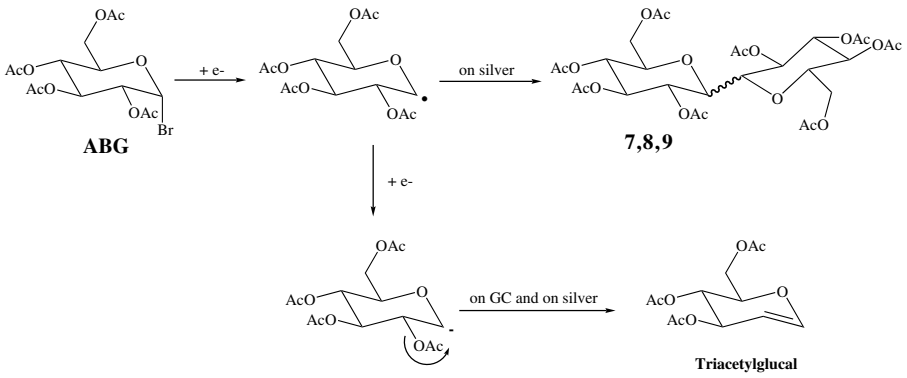

Scheme 2. Mechanism of electroreduction of **ABG**.

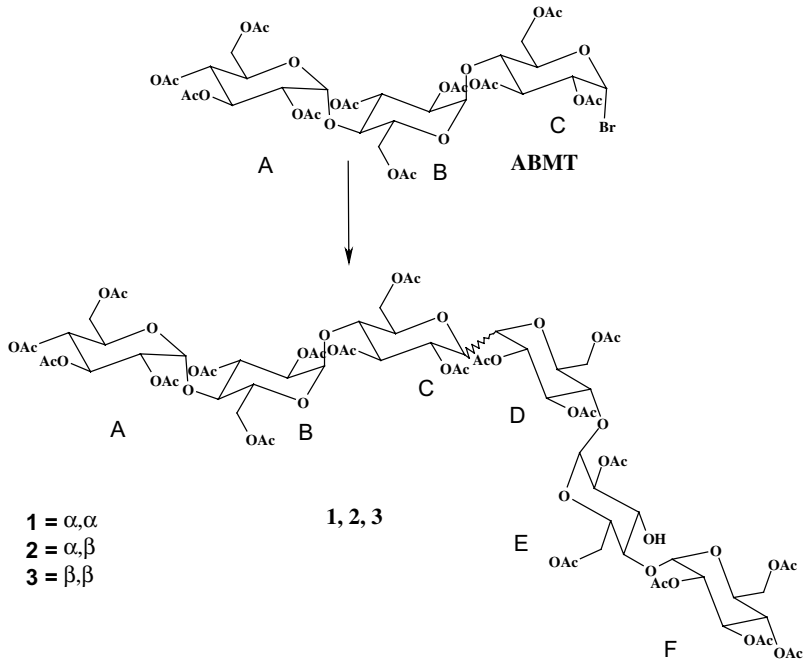

Scheme 3. Products coming from electroreduction of **ABMT**.

with metal ion induced dimerisation.[9] Glassy carbon probably has no specific interaction either with halosugars or with carbohydrate radicals that in fact mainly undergo further reduction. At the moment we can conclude that silver is the only electrode surface useful for our purposes. Apart from any speculations and synthetic limitations, the simplicity, the possibility of one-pot sugar unit doubling and the importance of glycomimetics in different biological applications prompted us to develop this electrochemical procedure.

The first goal presented in this paper is that peracetylated hexasaccharides as a mixture of diastereoisomers were successfully obtained by electroreduction of **ABMT** on silver (Scheme 3), although the reduction is more difficult passing from **ABG** and **ABM** to **ABTM** as evinced by E_p reported in Table 1. Probably the entropy requirements and steric hindrance due to the chain elongation are in part responsible for the more negative potential. We were able also to separate the three diastereoisomers **1**–**3** by flash silica gel chromatography. They were further purified on a HPLC semi-preparative column (Fig. 4) and were successfully and fully characterised by NMR spectroscopy with a great accuracy. NMR spectra of **2** reported in Figure 5, before and after purification, demonstrate the usefulness of the purification.

Deacetylation was carried out not only on **1**–**3,** but also on **7**–**9** and **13** and **14** to build up the library we had in mind. A concise presentation of the library is shown in Scheme 4, where *n* is the number of the glucose residue. NMR characterisation was successfully performed for all these new compounds with great accuracy, affording

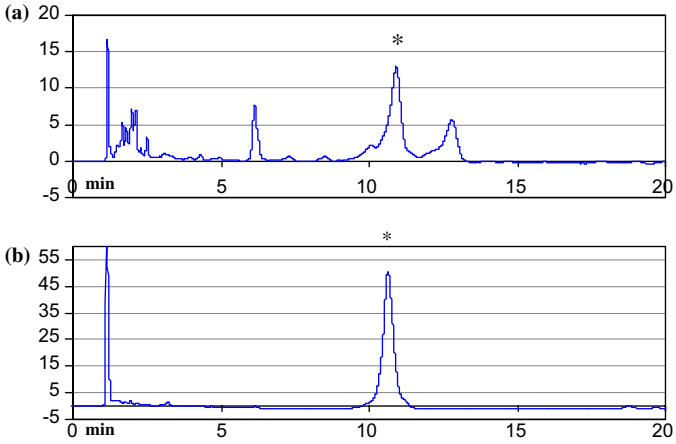

Figure 4. Chromatograms related to HPLC purification of **3**. (a) Crude fraction from silica gel flash chromatography enriched of the α,β peracetylated maltotriose dimer **3** (peak marked with *); (b) α,β Peracetylated maltotriose **3** dimer after semi-preparative HPLC purification.

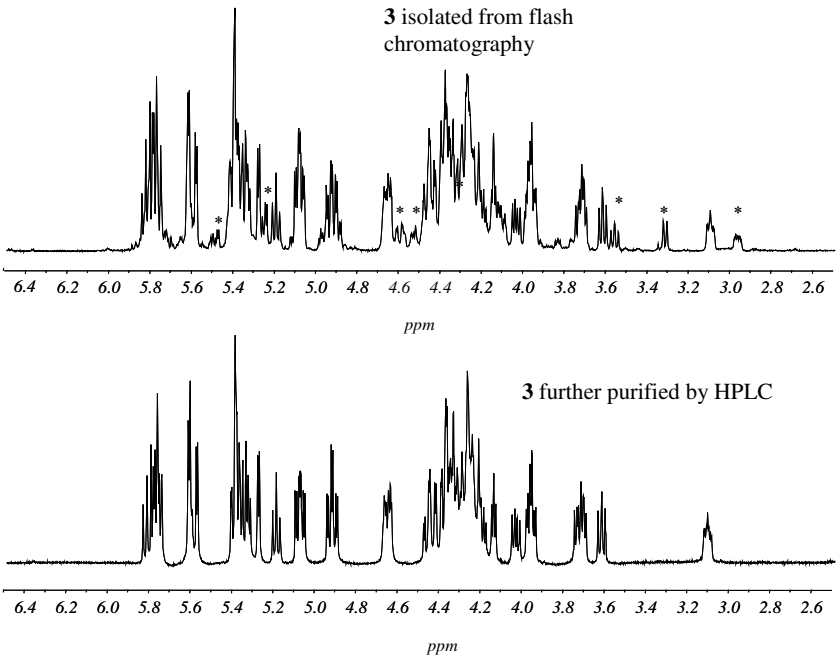

Figure 5. NMR spectra of **3** isolated and further purified on semi-preparative HPLC column, * indicates the signals that disappeared due to the purification.

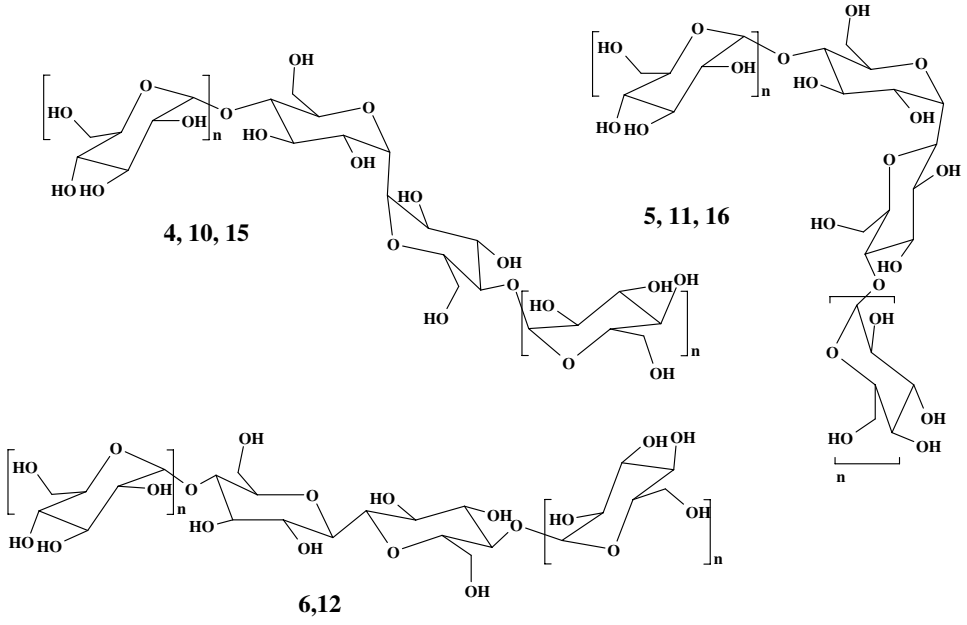

n = 0 ⇒ **10** (α,α) **11** (α,β) **12** (β,β)

n = 1 ⇒ **15** (α,α) **16** (α,β) not found (β,β)

n = 2 ⇒ **4** (α,α) **5** (α,β) **6** (β,β)

Scheme 4. Library of glucose-based glycomimetics from **ABG**, **ABM** and **ABMT**.

an important library of chemical shifts and coupling constants for unprotected sugar-based molecules.

As these new glucose-based skeletons, especially the hexasaccharide mimics, are suitable for biological applications, molecular modelling conformation analysis was carried out with the aim of investigating how the unusual *C*-interglycosidic bond influences the conformation and what roles the number of sugar units and the consequent chain elongation play.

2.2. Molecular modelling conformational analysis

Molecular modelling conformational analysis was performed on α,β compounds because only for these asymmetric products it is possible to measure the $J_{H1-H1'}$ NMR coupling constants, that have to be compared with theoretical results. Conformations of **5**, **11** and **16** were investigated by performing both 1D-Ramachandran plots and Monte Carlo/energy minimisation (MC/EM) conformational searches on models created using MACROMODEL version 7.1. Particular attention was put on *C*1–*H*1–*C*1′–*H*1′ torsional angles (θ) describing *C*-glycosidic bond conformation.

In 1D-Ramachandran plots of all the analysed compounds, three energy minima were found, corresponding to θ values of about 60°, 180° and 300°, respectively. In this view, we can define three family of conformers, differing in C–C bond glycosidic moiety orientation: *gauche*(+)- ($\theta = 60°$), *anti*- ($\theta = 180°$) and *gauche*(−) ($\theta = 300°$).

In order to evaluate convergence of calculations, two MC/EM simulations were carried out on each molecule, starting from models having *gauche*(+)- (MC1) and *gauche*(−)- (MC2) conformation. 30,000, 80,000 and 100,000 steps were run on **11**, **16** and **5**, respectively (Fig. 6). Results of each pair of simulations are in very good agreement (Table 2), indicating that all of them were convergent. Conformers found in MC/EM calculations of **11** explore all the three energetic minima individuated by 1D-Ramachandran plot with the same percentage distribution. On the contrary, more than 60% of conformers found out in MC/EM calculations of both **16** and **5** explored the minimum corresponding to *gauche*(−)-conformation. These different distributions prompted us to say that longer chains are accomplished by more rigid conformations.

In all the calculated structures, more than 90% of conformers of each minimum have $J_{H1-H1'}$ coupling constant values included within ranges shown in Table 3. Experimental $J_{H1-H1'}$ values measured on **16**, **11** and **5** are in good agreement with theoretical values $J_{H1-H1'}$ of both *gauche*(+)- and *gauche*(−)-C–C bond conformations. *gauche*(−) Conformation gives the best fitting with experimental data; for this reason it can be considered as the most probable C1–C1 bond conformation for **16**, **11** and **5** in water solution (Fig. 7).

In the conformational analysis of **16** and **5**, geometries of glycosidic dihedral angles ϕ and ψ were evaluated. In most of the conformations individuated by MC/EM simulations of both compounds, ϕ and ψ range from 300° to 350° and from 270° to 360°, respectively. NMR, optical rotation and computational analysis on maltose in water solution[10] indicated that maltose distributes between the states $\phi = 290°$, $\psi = 320°$ and $\phi = 330°$, $\psi = 345°$. Therefore, we can observe that in both 1α-(β′-maltosyl)-1,5-anhydro-maltitol **11** and 1α-(β′-maltotriosyl)-1,5-anhydro-maltotritol **5** the *O*-glucosidic linkages seem to maintain the same conformation of O-linked maltosides. Indeed, the presence of an unusual C–

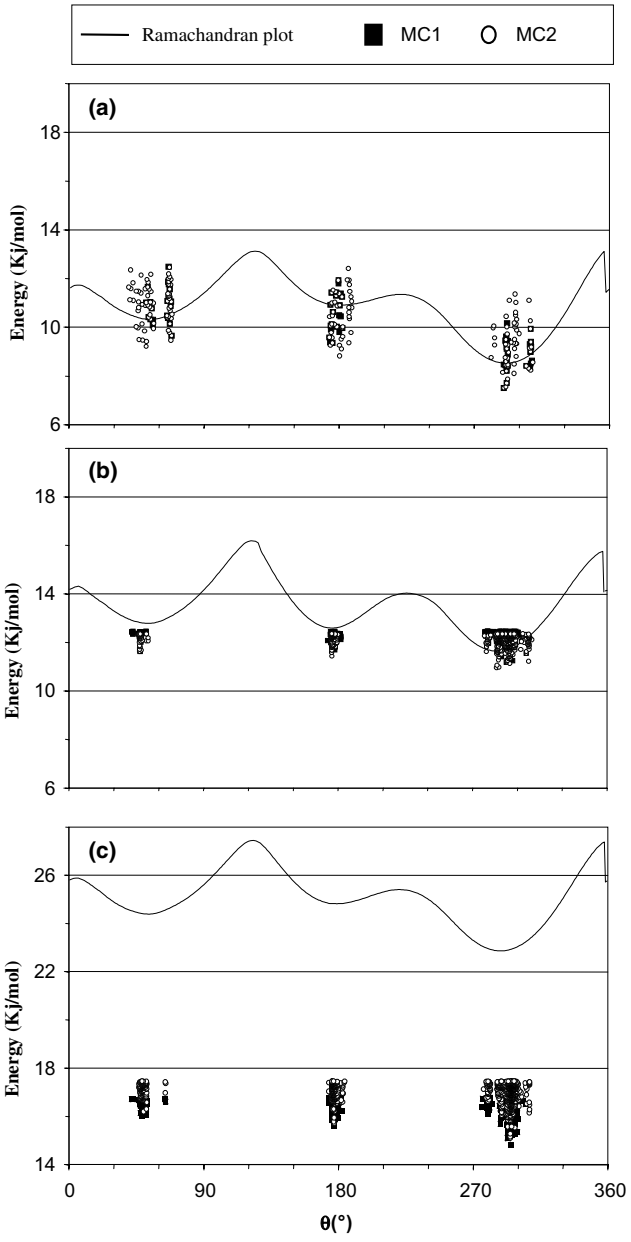

Figure 6. 1D-Ramachandran maps and MC scatter plots of θ torsional angle of compounds **11** (a), **16** (b) and **5** (c).

Table 2. Percentage distribution of conformers found out by MC/EM conformational searches on **16**, **11** and **5**

		gauche(+) (%)	*anti* (%)	*gauche*(−) (%)
11	MC 1	34	31	35
	MC 2	31	31	38
16	MC 1	14	20	66
	MC 2	13	19	68
5	MC 1	13	23	65
	MC 2	12	22	66

Percentage distribution of conformers found out by MC/EM conformational searches on **11**, **16** and **5** molecular models in the three minima centered on $\theta = 60°$ (*gauche*(+)), $\theta = 180°$ (*anti*) and $\theta = 300°$ (*gauche*(−)), respectively. Two simulations were performed on each compound, starting from *gauche*(+)- (MC 1) and *gauche*(−)- (MC 2) conformers.

Table 3. Comparison between experimental and theoretical H1–H1′ coupling constants

	Experimental $J_{H1-H1'}$ (Hz)	Theoretical $J_{H1-H1'}$ *gauche*(+) (Hz)	Theoretical $J_{H1-H1'}$ *anti* (Hz)	Theoretical $J_{H1-H1'}$ *gauche*(−) (Hz)
11	1.4			
16	2.5	2.4–4.9	9.6–9.8	0.7–2.9
5	2.2			

Experimental $J_{H1-H1'}$ values measured on compounds **11**, **16** and **5** and theoretical $J_{H1-H1'}$ ranges including more than 90% of *gauche*(+), *anti* and *gauche*(−) conformers individuated by MC/EM simulations performed on the same compounds.

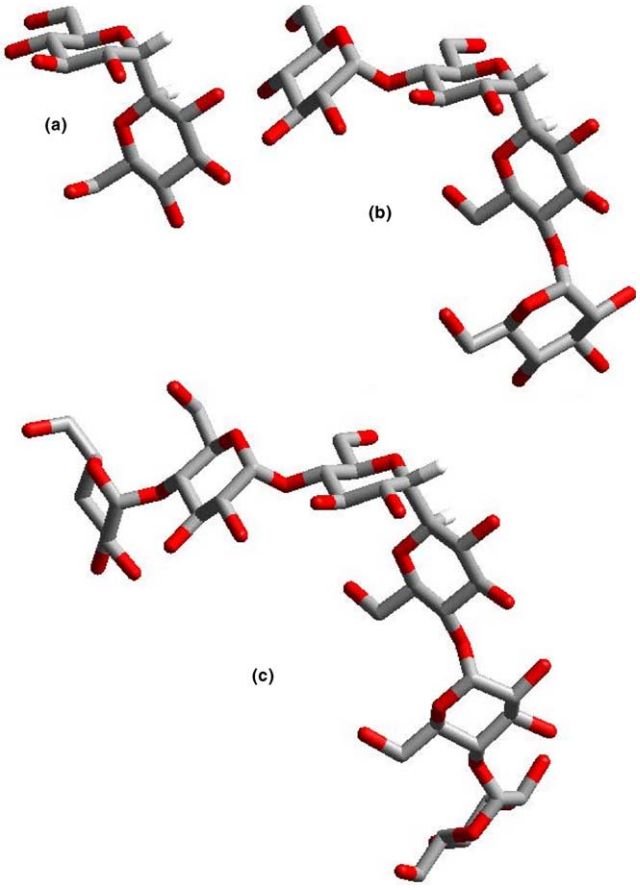

Figure 7. *gauche*(−)-Conformers of **11** (a), **16** (b) and **5** (c).

C linkage of the parent reducing residues of these asymmetrical diastereoisomers involves a drastic distorsion of the chain conformation of 1–4 α-maltooligosaccharides, as shown superimposing preferred conformation c (Fig. 8) of **5** with the most probable conformation of maltohexaose.

3. Conclusion

An original library of potential glycomimetics including glucose-based compounds of two, four and six units characterised by one direct *C*-interglycosidic bond, was built by a clean and simple approach, the electroreduction of the parent bromo sugars, that is a one-pot radical pathway to double parent sugar units. The three diastereoisomers built up between the new *C*-interglycosidic bond show a prevalent *gauche* conformation characterised by a drastic distorsion respect to the regular *O*-glucosidic bond.

4. Experimental

4.1. General procedures

Peracetylated maltotriose was produced by known methods. All other reagents and solvents were purchased from Sigma–Aldrich. They were of reagent grade and used without further purification. Reaction were monitored by TLC visualising by charring with 10% H_2SO_4 in water. Cyclic voltammetry experiment was carried out with an Amel 2053 potentiostat coupled with an Amel 7800 function generator. Cell temperature: 20 °C, sample concn: 4 mM in ACN. Preparative electrolyses were carried out with the Amel 553 potentiostat. Analytical HPLC were performed with a 1100 series Agilent HPLC instrument. Column: Hypersil BDS C18 250 × 4.6 mm from Agilent Technologies. Rheodine valve volume: 20 μL. Eluent: 55% acetonitrile/45% water. Flow rate: 1.5 mL/min. Detection by UV at 210 nm. Samples were dissolved in ACN at the concentration of 1 mg/mL; 20 μL were injected. Semi preparative HPLC was performed in the same conditions, using an Hypersil BDS C18 250 × 10 mm column from Thermo Hypersil, a Rheodine valve of 100 μL and a flow rate of 5 mL/min. Samples were dissolved in ACN at the concentration of 100 mg/mL; 70 μL were injected. ^{13}C NMR and ^{1}H NMR spectra were recorded at 500 MHz for ^{1}H and 125 MHz for ^{13}C with a Bruker AMX 500 spectrometer equipped with a 5 mm $^{1}H/X$ inverse probe. Acetylated samples (10 mg) were dissolved in benzene-d_6 (0.6 mL, 99.96% D) and analysed at 303 K; chemical shift are expressed in ppm downfield from TMS. Deprotected samples (10 mg) were dissolved in D_2O and lyophilised. The operation was repeated three times, then samples were dissolved in D_2O (0.6 mL, 99.99% D) and analysed; chemical shift are expressed in ppm downfield from sodium 3-(trimethylsilyl)propionate. Assignments were made trough HMQC, COSY and TOCSY experiments. MALDI-TOF MS were acquired on a BIFLEX (Bruker) operating in the positive ion reflector mode. Ions, formed by a pulsed UV laser beam (nitrogen laser, $\lambda = 337$ nm) were accelerated at 19 keV. 2,5-DHB (10 mg/mL in ACN) was used as matrix, 5 μL of the sample dissolved in ACN (concn 20–40 pmol/μL) were added to 5 μL of matrix solution and 1 μL was deposited on the target. External calibration was performed with angiotensin II peptide. Electron spray ionisation MS (ESI/MS) and ESI-MS/MS experiments were performed in positive or negative ion mode with a Esquire 3000 Plus ion trap (Bruker) using the following instrumental parameters: source voltage: 4.0 kV, nebuliser gas 12 psi, dry gas flow rate 4 L/min at 280 °C, capillary voltage 160 V. Samples were sprayed by flow injection analysis at 4 μL/min at a concentration of 20–50 pmol/μL in ACN for protected analytes and in ACN/H_2O (1:1, v/v) with 10 mM

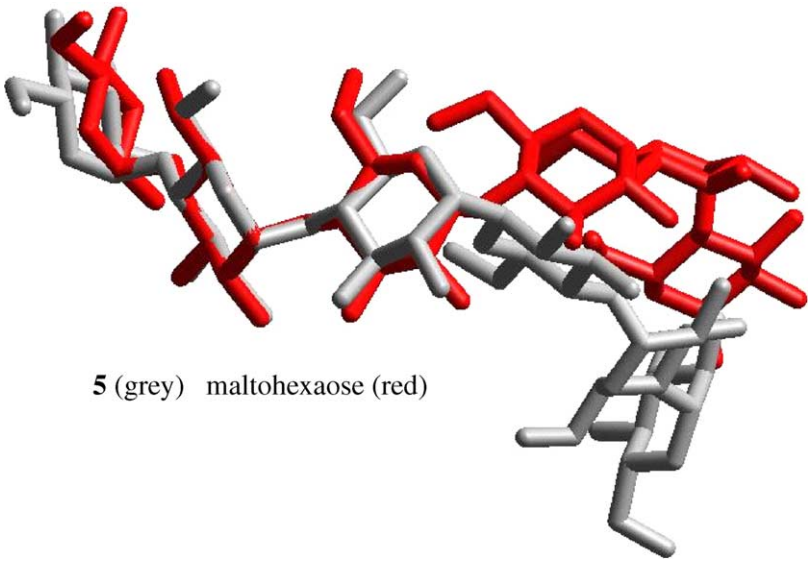

Figure 8. Conformation (c) of **5** superimposed on maltohexaose.

ammonium acetate for deprotected samples. MS/MS experiments were performed using an isolation width of 4 Da and amplitude fragmentation of 1 V for 40 ms. Melting points were measured with a 10× magnification Reichert microscope equipped with an heating plate and are not corrected. Optical rotations were measured on a Dr. Kernichen Propol digital automatic polarimeter.

4.1.1. 2,3,4,6-Tetra-*O*-acetyl-α-D-glucopyranosyl-(1→4)-2,3,6-tri-*O*-acetyl-α-D-glucopyranosyl-(1→4)-2,3,6-tri-*O*-acetyl-β-D-glucopyranosyl-bromide ABMT. HBr solution (18.5 mL, 39%) in CH_3COOH were added at 0 °C to 6.16 g (6.38 mmol) of peracetylated maltotriose dissolved in 30 mL of anhydrous methylene chloride. After stirring at 0 °C for 1.5 h the mixture was diluted with 100 mL of CH_2Cl_2, washed subsequently with cold water, $NaHCO_3$ saturated water and again with water. After solvent removal, the residue was flash chromatographed on silica gel with 6:4 AcOEt/hexane obtaining 6.17 g of **ABMT** as a white solid in a 98% yield. Crystallised from EtOH. Mp: 103 °C. MALDI: *m/z* 1011.3 [M+Na$^+$], 1025.2 [M+K$^+$]. ^{1}H NMR (C_6D_6, three rings are termed for convenience: ABC–Br): 1.59–1.92 (m, 30H, CH_3CO) 3.76 (dd, $J_{6aC–5C}$ = 3.4, $J_{6aC–6bC}$ = 12.8, H-6aC); 3.93 (dd); 3.99 (dt, H-5B); 4.02 (dt, H-5C); 4.06 (dd); 4.17 (dd, $J_{6bC–5C}$ = 2.6, $J_{6bC–6aC}$ = 12.8, H-6bC); 4.25 (dt, H-5A); 4.29 (dd, $J_{6aB–5B}$ = 3.1, $J_{6aB–6bB}$ = 12.4, H-6aB); 4.38 (dd, $J_{6aA–5A}$ = 1.9, $J_{6aA–6bB}$ = 12.5, H-6aA); 4.47 (H-6bA); 4.64 (dd, $J_{2C–1C}$ = 3.9, $J_{2C–3C}$ = 9.7, H-2C); 4.66 (dd, $J_{6bB–5B}$ = 2.8, $J_{6bB–6aB}$ = 12.4, H-6bB); 4.90 (dd, $J_{2B–1B}$ = 4.0, $J_{2B–3B}$ = 10.5, H-2B); 5.08 (dd, $J_{2A–1A}$ = 3.9, $J_{2A–3A}$ = 10.5, H-2A); 5.40 (d, $J_{1B–2B}$ = 4.0, H-1B); 5.42 (t, $J_{4A–3A}$ = 9.0, $J_{4A–5A}$ = 9.0, H-4A); 5.66 (d, $J_{1A–2A}$ = 3.9, H-1A); 5.85 (m, H-3A); 5.86 (m, H-3B, H-3C); 6.24 (d, $J_{1C–2C}$ = 3.9, H-1C). ^{13}C NMR (C_6D_6): 20.6–21.0 (*C*H_3CO) 62.6 (C-6aB, C-6bB); 61.8 (C-6aA, C-6bA, C-6aC, C-6bC); 68.8 (C-4A); 69.3 (C-5A); 69.7 (C-3A); 69.8 (C-5B); 70.7 (C-2A); 70.9 (C-2B); 71.3 (C-2C); 72.1–73.1 (C-3B, C-3C); 72.7–73.0 (C-4B, C-4C); 73.0 (C-5C); 87.0 (C-1C); 96.1 (C-1A); 96.4 (C-1B); 169.7–171.1 (CH$_3$*C*O).

4.2. Preparative electroreduction of ABMT

The electrolysis was carried out under potentiostatic condition at room temperature under nitrogen atmosphere in a two-compartment cell, divided with an anion-exchange membrane. Cathodic solution (50 mL) made by anhydrous acetonitrile and containing 1.15 g of tetraethylammonium perchlorate (TeaP) as supporting electrolyte were pre-electrolysed 10 min between −1.0 V and −1.9 V, using a silver plate as cathode and a silver plate as anode in 50 mL of anhydrous acetonitrile saturated with tetraethylammonium bromide. A Sybron membrane was used to separate anodic and cathodic compartments. After the pre-electrolysis, 5.82 g (5.89 mmol) of **ABMT** were added to the cathodic solution and were exhaustively electrolysed at −1.600 V. The solution at the cathodic compartment was concentrated and precipitated with AcOEt. The solid supporting electrolyte was filtered off. The filtrate was evaporated at reduced pressure and the residue was chromatographed on silica gel from 4:6 hexane/acetate to acetate, obtaining a crude mixture of α,α, α,β and β,β isomers (34% yields). After a second chromatography in the same conditions, fractions enriched in single isomer were obtained. These fractions were purified through semi-preparative HPLC yielding pure isomers of peracetylated 1α-(α′-maltotriosyl)-1,5-anhydro-maltotritol **1**, 1α-(β′-maltotriosyl)-1,5-anhydro-maltotritol **2** and 1β-(β′-maltotriosyl)-1,5-anhydro-maltotritol **3**.

4.2.1. Compound 1 (α,α isomer). Tr (analytical column, ID = 4.6 mm): 9.74 min. Mp = 120 °C. $[\alpha]_D^{25}$ = +101.4 (*c* 0.5, $CHCl_3$). MALDI-MS: *m/z* = 1837.4 [M+Na$^+$], 1853.4 [M+K$^+$]. ^{1}H NMR (C_6D_6, six rings are termed for convenience: ABC–CBA): 1.62–2.11 (m, 60H, CH_3CO), 3.76 (dd, $J_{4C–3C}$ = 4.2, $J_{4C–5C}$ = 7.7, H-4C); 3.94 (dd, $J_{4B–3B}$ = 9.1, $J_{4B–5B}$ = 9.9, H-4B); 4.10 (m, H-5C); 4.12 (m, C-6aC); 4.21 (dt, $J_{5B–4B}$ = 10.0, $J_{5B–6aB}$ = 3.4, $J_{5B–6bB}$ = 3.4, H-5B); 4.27 (m, H-5A); 4.29 (dd, $J_{6aB–5B}$ = 4.0, $J_{6aB–6bB}$ = 12.3, H-6aB); 4.38 (dd, $J_{6aA–5}$ = 2.4, $J_{6aA–6bA}$ = 12.3, H-6aA); 4.44 (m, H-6bC); 4.45

(m, H-6bA); 4.57 (s, H-1C); 4.65 (dd, J_{6bB-5B} = 2.8, $J_{6bB-6aB}$ = 12.3, H-6bB); 4.97 (dd, J_{2B-1B} = 3.9, J_{2B-3B} = 10.4, H-2B); 5.08 (dd, J_{2A-1A} = 4.0, J_{2A-3A} = 10.5, H-2A); 5.30 (m, H-2C); 5.392 from monodimensional ^{1}H spectrum (d, J_{1B-2B} = 3.9, H-1B); 5.395 from monodimensional ^{1}H spectrum (t, J_{4A-5A} = 9.7, J_{4A-5A} = 9.7, H-4A); 5.42 (dd, J_{3C-2C} = 5.8, J_{3C-4C} = 4.2, H-3C); 5.58 (d, J_{1A-2A} = 4.0, H-1A); 5.73 (dd, J_{3B-2B} = 10.4, J_{3B-4B} = 9.1, H-3B); 5.78 (dd, J_{3A-2A} = 10.5, J_{3A-4A} = 9.4, H-3A). ^{13}C NMR (C_6D_6): 61.6 (C-6aA, C-6bA); 62.8 (C-6aB, C-6bB); 63.3 (C-6aC, C-6bC); 68.5 (C-4A); 68.9 (C-1C); 69.0 (C-5A); 69.3 (C-5B); 69.4 (C-2C); 69.7 (C-3A); 70.7 (C-2A, C-2B); 71.1 (C-3C); 72.0 (C-5C); 72.2 (C-3B); 73.4 (C-4B); 75.4 (C-4C); 96.1 (C-1A); 97.0 (C-1B).

4.2.2. Compound 2 (α,β isomer). Tr (analytical column, ID = 4.6 mm): 10.49 min. Mp = 123 °C; $[\alpha]_D^{25}$ = +98.2 (*c* 1, $CHCl_3$); ESI-MS: *m*/*z* = 1837.5 [M+Na$^+$], 1853.4 [M+K$^+$]. ^{1}H NMR (C_6D_6, six rings are termed for convenience: ABC–DEF): 1.59–2.24 (m, 60H, C*H*$_3$CO) 3.10 (ddd, J_{5D-4D} = 9.6, J_{5D-6aD} = 6.3, J_{5D-6bD} = 2.6, H-5D); 3.62 (dd, J_{4D-3D} = 8.2, J_{4D-5D} = 9.6, H-4D); 3.71 (m, H-4C); 3.74 (m, H-1D); 3.96 (m, H-4B, H-4E); 4.03 (dd, J_{6aD-5D} = 6.3, $J_{6aD-6bD}$ = 12.1, H-6aD); 4.15 (m, H-1C); 4.23–4.23 (m, H-5B, H-5E); 4.25 (m, H-6bD); 4.26 (m, H-5C); 4.39 (m, H-6aA, H-6aB); 4.46 (m, H-6bA, H-6bB); 4.22–4.66 (m, H-6aB, H-6bB, H-6aE, H-6bE, H-6aC, H-6bC), 4.93 (dd, J_{2B-1B} = 3.9, J_{2B-3B} = 10.8, J_{2E-1E} = 3.9, J_{2E-3E} = 10.8, H-2B, H-2E); 5.09 (dd, J_{2A-1A} = 3.9, J_{2A-3A} = 9.2, J_{2F-1F} = 3.9, J_{2F-3F} = 9.2, H-2A, H-2F); 5.20 (t, J_{2D-1D} = 8.9, J_{2D-3D} = 8.9, H-2D); 5.28 (d, J_{1E-2E} = 3.9, H-1E); 5.33 (m, H-2C); 5.36 (m, H-3D); 5.39 (m, H-1B); 5.40 (m, H-4A, H-4F); 5.58 (d, J_{1A-2A} = 3.9, H-1A); 5.62 (m, H-1F, H-3C); 5.82–5.75 (m, H-3B, H-3E); 5.79 (m, H-3A, H-3F). ^{13}C NMR (C_6D_6): 61.6 (C-6aA, C-6bA, C-6aF, C-6bF); 62.7 (C-6aB, C-6bB, C-6aC, C-6bC C-6aE, C-6bE); 63.6 (C-6aD, C-6bD); 68.0 (C-2C); 68.5 (C-4A, C-4F); 68.9–69.4 (C-5A, C-5B, C-5E, C-5F); 69.6 (C-3A, C-3F); 70.5 (C-1C, C-3C); 70.6 (C-2A, C-2F); 70.7 (C-2B, C-2E); 70.8 (C-2D); 71.9–72.0 (C-3B, C-3E); 72.8 (C-5C); 73.2 (C-4B, C-4E); 74.6 (C-4D); 74.8 (C-4C); 76.0 (C-3D, C-5D); 76.4 (C-1D); 95.8 (C-1F); 96.0 (C-1A); 96.2 (C-1E); 96.8 (C-1B).

4.2.3. Compound 3 (β,β isomer). Tr (analytical column, ID = 4.6 mm): 12.84 min. ESI-MS: *m*/*z* = 1873.5 [M+Na$^+$], 1853.4 [M+K$^+$]. ^{1}H NMR (C_6D_6, six rings are termed for convenience: ABC–CBA): 1.65–1.94 (m, 60H, C*H*$_3$CO), 2.97 (ddd, J_{5C-4C} = 9.8, J_{5C-6aC} = 5.0, J_{5C-6bC} = 3.0, H5-C); 3.31 (d, J_{1C-2C} = 8.8, H-1C); 3.55 (dd, J_{4C-3C} = 8.2, J_{4C-5C} = 9.8, H-4C); 3.95 (dd, J_{6aC-5A} = 5.0; $J_{6aC-6bC}$ = 12.1, H-6aC); 3.96 (t, J_{4B-3B} = 9.4, J_{4B-5B} = 9.4, H-4B); 4.08 (dt, J_{5A-4A} = 9.8, J_{5A-6aA} = 3.1, J_{5A-6bA} = 3.1, H-5A); 4.12 (dd, J_{6bB-5B} = 3.0, $J_{6bB-6aB}$ = 12.1, H-6bC); 4.24 (dt, J_{5B-4B} = 10.2, J_{5B-6aB} = 3.1, J_{5B-6bB} = 3.1, H-5B); 4.27 (dd, J_{6aB-5B} = 3.6, $J_{6aB-6bB}$ = 12.4, H-6aB); 4.35 (dd, J_{6aA-5A} = 2.6, $J_{6aA-6bA}$ = 12.4, H-6aA); 4.44 (dd, J_{6bA-5A} = 3.7, $J_{6bA-6aA}$ = 12.4, H-6bA); 4.57 (dd, J_{6bB-5B} = 2.9, $J_{6bB-6aB}$ = 12.4, H-6bB); 4.87 (dd, J_{2B-1B} = 3.9, J_{2B-3B} = 10.4, H-2B); 5.05 (dd, J_{2A-1A} = 3.9, J_{2A-3A} = 10.4, H-2A); 5.22 (d, J_{1B-2B} = 3.9, H-1B); 5.31 (m, H-2C); 5.37 (m, H-4A, H-3C); 5.59 (d, J_{1A-2A} = 3.9, H-1A); 5.77 (dd, J_{3A-2A} = 10.4, J_{3A-4A} = 9.6, H-3A); 5.78 (dd, J_{3B-2B} = 10.4, J_{3B-4B} = 8.9, H-3B). ^{13}C NMR (C_6D_6): 61.6 (C-6aA, C-6bA); 62.6 (C-6aB, C-6bB); 63.2 (C-6aC, C6bC); 68.4 (C-2C); 68.5 (C-4A); 68.9 (C-5B); 69.3 (C-5A); 69.6 (C-3A); 70.6 (C-2A); 70.7 (C-2B); 71.8 (C-3B); 73.1 (C-4B); 73.9 (C-1C); 74.2 (C-4C); 76.5 (C-5C); 77.6 (C-3C); 95.8 (C-1A); 96.1 (C-1B).

4.3. Deacetylation of peracetylated compounds coming from ABG, ABM and ABMT

4.3.1. 1α-(α′-Maltotriosyl)-1,5-anhydro-maltotritol 4. Compound **1** (97 mg, 0.053 mmol) and 5.9 mL of 0.2 M MeONa in MeOH were stirred overnight at rt. An equal volume of water was added and pH was adjusted to 7 with Amberlite IR-120 (H$^+$ form). The resin was filtered off and solvent was removed. After size exclusion chromatography on Sephadex G25 resin compound **4** was obtained as a white solid in quantitative yield. $[\alpha]_D^{25}$ = +147.3 (*c* 0.33, H_2O); ESI-MS: *m*/*z* = 992.4 [M+NH_4^+], 997.3 [M+Na$^+$], 1013.3 [M+ K$^+$], MS/MS (992.4): *m*/*z* = 975.3 [M+H]$^+$, 813.2, 651.2, 489.1. ^{1}H NMR (D_2O, six rings are termed for convenience: ABC–CBA): 3.42 (t, J_{4A-3A} = 9.5, J_{4A-5A} = 9.5, H-4A); 3.59 (dd, J_{2A-1A} = 3.9, J_{2A-3A} = 9.9, H-2A); 3.63 (dd, J_{2B-1B} = 3.9, J_{2B-3B} = 9.9, H-2B); 3.66 (t, J_{4B-3B} = 9.3, J_{4B-5B} = 9.3, H-4B); 3.69 (t, J_{3A-2A} = 9.4, J_{3A-4A} = 9.4, H-3A); 3.72 (m, H-5A); 3.75 (m, H-4C, H-6aC); 3.75–3.89 (m, H-6aA, H-6bA, H-6aB, H-6bB); 3.83 (m, H-5B); 3.89 (m, H-2C); 3.99 (m, H-3B); 4.01 (m, H-6bC); 4.08 (ddd, H-5C); 4.10 (t, J_{3C-2C} = 5.3, J_{3C-4C} = 5.3, H-3C); 4.31 (s, H-1C); 5.25 (d, J_{1B-2B} = 3.9, H-1B); 5.39 (d, J_{1A-2A} = 3.9, H-1A). ^{13}C NMR (D_2O): 62.2 (C-6aC, C-6bC); 63.4 (C-6aA, C-6bA, C6aB, C6bB); 71.8 (C-2C); 71.9 (C-1C); 72.0 (C-3C); 72.2 (C-4A); 74.0 (C-2B, C-5B); 74.6 (C-2A); 75.6 (C-5A); 75.8 (C-3A); 76.2 (C-3B); 76.8 (C-4C); 79.6 (C-5C); 79.8 (C-4B); 100.9 (C-1B); 102.6 (C-1A).

4.3.2. 1α-(β′-Maltotriosyl)-1,5-anhydro-maltotritol 5. Compound **2** (73 mg, 0.040 mmol) was deprotected to compound **5** in quantitative yield, as above described for **4**. ESI-MS: *m*/*z* = 973.3 [M−H]$^-$. ^{1}H NMR (D_2O, six rings are termed for convenience: ABC–DEF): 3.42 (m, H-4A, H-4F); 3.53 (ddd, J_{5D-4D} = 9.6, J_{5D-6aD} = 2.1, J_{5D-6bD} = 5.0, H-5D); 3.58 (m, H-2A, H-2F); 3.61 (m, H-4C); 3.61–3.62 (m, H-2B,H-2E); 3.65 (m, H-4B, H-4D, H-4E); 3.69 (m, H-3A, H-3F); 3.73 (m, H-5A, H-5F); 3.69 (m, H-1D, H-2D); 3.72 (m, H-3D); 3.74–3.88 (m, H-6aA, H6bA, H-6aB, H-6bB, H-6aE, H-6bE, H-6aF, H-6bF); 3.79 (m, H-6aD); 3.82 (m, H-6aC); 3.84 (m, H5B, H-5E); 3.85 (m, H-6bC); 3.92 (m, H-2C); 3.93 (m, H-6bD); 3.97 (m, H-3B, H-3E); 4.04 (m, H-5C); 4.28 (dd, J_{1C-1D} = 2.2, J_{1C-2C} = 5.1, H-1C); 4.31 (m, H-3C); 5.28 (d, J_{1B-2B} = 3.9, H-1B); 5.38 (d, J_{1A-2A} = 3.9, J_{1F-2F} = 3.9, H-1A, H-1F), 5.39 (J_{1F-2F} = 3.9, H-1F). ^{13}C NMR (D_2O): 63.1 (C-6aC, C-6bC) 63.4 (C-6aA, C-6bA, C-6aB, C-6bB, C-6aE, C-6bE, C-6aF, C-6bF); 63.8 (C-6aD, C-6bD); 72.2 (C-4A, C-4F); 73.3 (C-2C); 74.0 (C-5B, C-1C, C-5E); 74.3 (C-2B, C-2E); 74.6 (C-3C, C-2A, C-2F); 72.2–74.4 (C-2B, C-2E);

75.7 (C-3A, C-3F); 76.2 (C-3B, C3E); 78.4 (C-5C); 79.2 (C-4C); 79.7 (C-4B, C-4D, C-4E); 80.9 (C-3D); 81.1 (C-5D); 83.8 (C-1D); 101.4 (C-1B); 102.4 (C-1E); 102.6 (C-1A, C-1F).

4.3.3. 1β-(β′-Maltotriosyl)-1,5-anhydro-maltotritol 6. Compound **3** (73 mg, 0.040 mmol) was deprotected to compound **6** in quantitative yield, as above described for **4**. ESI-MS: $m/z = 992.4$ [M+NH_4^+], 997.3 [M+Na^+], 1013.3 [M+K^+], MS/MS (992.4): $m/z = 975.3$ [M+H]$^+$, 813.3, 651.2, 489.1; ^{1}H NMR (D_2O, six rings are termed for convenience: ABC–CBA): 3.42 (t, $J_{4A–3A} = 9.4$, $J_{4A–5A} = 9.4$, H-4A); 3.53 (ddd, $J_{5C–4C} = 9.8$, $J_{5C–6aC} = 5.3$, $J_{5C–6bC} = 2.0$, H-5C); 3.58 (m, H-2A, H-4C); 3.59 (m, H-1C); 3.63 (m, H-2B); 3.64 (m, H-4B); 3.67 (m, H-3A); 3.70 (m, H-2C); 3.72 (m, H-5A); 3.74 (m, H-6aC); 3.74–3.88 (m, H-6aA, H-6bA, H-6aB, H-6bB); 3.80 (m, H-3C); 3.84 (m, H-5B); 3.93 (dd, $J_{6bC–6aC} = 12.5$, $J_{6bC–5C} = 2.0$, H-6bC); 3.96 (dd, H-3B); 5.38 (d, $J_{1A–2A} = 3.7$, $J_{1B–2B} = 3.7$, H-1A, H-1B). ^{13}C NMR (D_2O): 63.4 (C-6aA, C-6bA, C6aB, C6bB); 63.8 (C-6aC, C-6bC); 71.1 (C-2C); 72.2 (C-4A); 74.1 (C-5B); 74.4 (C-2B); 74.6 (C-2A); 75.6 (C-5A); 75.7 (C-3A); 76.2 (C-3B); 78.4 (C-1C); 79.9 (C-4B); 80.4 (C-4C); 80.7 (C-3C); 81.4 (C-5C); 102.6 (C-1A, C-1B).

4.3.4. 1α-(α′-Glucosyl)-1,5-anhydro-glucitol 10. Compound **7** (15 mg, 0.023 mmol) was deprotected as described for compound **4** obtaining **10** in quantitative yield. ESI-MS: $m/z = 325.0$ [M−H]$^-$, MS/MS (325.0): $m/z = 325.0$, 306.9, 228.9, 205.0, 186.9, 139.0. ^{1}H NMR (D_2O): 3.38 (m, H-4); 3.68 (m, H-6a, H-6b); 3.69 (m, H-3); 3.74 (m, H-2, H-5); 4.27 (d, $J_{1–2} = 3.2$, H-1). ^{13}C NMR (D_2O): 63.2 (C-6); 71.9 (t, $J_{4–3} = 8.1$, $J_{4–5} = 8.1$, C-4); 73.0 (C-1); 73.7 (C-2); 75.9 (C-3); 78.9 (C-5).

4.3.5. 1α-(β′-Glucosyl)-1,5-anhydro-glucitol 11. Compound **8** (22 mg, 0.033 mmol) was deprotected as described for compound **4** obtaining **11** in quantitative yield. ESI-MS: $m/z = 325.0$ [M−H]$^-$, MS/MS (325.0): $m/z = 325.0$, 306.9, 228.9, 186.9, 139.0. ^{1}H NMR (D_2O, two rings are termed for convenience: A–B): 3.37 (dd, $J_{4A–3A} = 8.4$, $J_{4A–5A} = 9.4$, H-4A); 3.41 (m, H-5B); 3.43 (m, H-3B); 3.45 (t, $J_{4B–5B} = 8.5$, $J_{4B–5B} = 8.5$, H-4B); 3.67 (dd, $J_{6aA–5A} = 6.4$, $J_{6aA–6bA} = 12.3$, C-6aA); 3.69 (m, H-2B); 3.70 (m, H-1B); 3.76 (dd, $J_{6aB–5B} = 4.8$, $J_{6aB–6bB} = 12.4$, C-6aB); 3.83 (dd, $J_{6bA–5A} = 2.4$, $J_{6bA–6aA} = 12.3$, C-6bA); 3.87 (m, H-2A); 3.88 (m, H-5A); 3.91 ($J_{6bB–5B} = 2.1$, $J_{6bB–6aB} = 12.4$, H-6bB); 4.13 (t, $J_{3A–2A} = 8.9$, $J_{3A–4A} = 8.4$, H-3A); 4.35 (dd, $J_{1A–2A} = 6.5$, $J_{1A–1B} = 1.4$, H-1A). ^{13}C NMR (D_2O): 63.8 (C-6aB, C-6bB); 64.0 (C-6aA, C-6bA); 72.1 (C-4B); 73.2 (C-4A); 74.5 (C-2B); 74.8 (C-2A); 75.0 (C-1A); 76.9 (C-3A); 78.8 (C-5A); 80.8 (C-3B); 82.7 (C-5B); 86.1 (C-1B).

4.3.6. 1-β-(β′-Glucosyl)-1,5-anhydro-glucitol 12. Compound **9** (20 mg, 0.030 mmol) was deprotected as described for compound **4** obtaining Compound **12** in quantitative yield. ESI-MS: $m/z = 325.0$ [M−H]$^-$, MS/MS (325.0): $m/z = 325.1$, 306.9, 204.9, 139.0. ^{1}H NMR (D_2O): 3.35 (dd, $J_{4–3} = 8.8$, $J_{4–5} = 9.8$, H-4); 3.40 (ddd, $J_{5–4} = 9.8$, $J_{5–6a} = 5.9$, $J_{5–6b} = 2.2$, H-5); 3.52 (t, $J_{3–2} = 8.9$, $J_{3–4} = 8.9$, H-3); 3.59 (d, $J_{1–2} = 9.4$, H-1); 3.67 (t, $J_{2–1} = 9.3$, $J_{2–3} = 8.9$, H-2); 3.70 (dd, $J_{6a–5} = 5.9$, $J_{6a–6b} = 12.4$, H-6a); 3.90 (dd, $J_{6b–5} = 2.2$, $J_{6b–6a} = 12.4$, H-6b). ^{13}C NMR (D_2O): 63.9 (C-6a, C-6b); 71.3 (C-2); 72.7 (C4); 78.5 (C1); 80.4 (C3); 82.8 (C5).

4.3.7. 1α-(α′-Maltosyl)-1,5-anhydro-maltitol 15. Compound **13** (329 mg, 0.266 mmol) was deprotected as described for compound **4** obtaining **15** in a quantitative yield. MALDI-MS: $m/z = 673$ [M+Na^+], 689 [M+K^+]. ^{1}H NMR (D_2O, four rings are termed for convenience: AB–BA): 3.43 (t, $J_{4A–3A} = 9.6$, $J_{4A–5A} = 9.6$, H-4A); 3.59 (dd, $J_{2A–1A} = 3.9$, $J_{2A–3A} = 9.8$, H-2A); 3.72–3.75 (m, H-3A, H-5A, H-4B); 3.76 (dd, $J_{6aB–6bB} = 12.4$, $J_{6aB–5B} = 2.2$, H-6aB); 3.77 (m, H-6aA); 3.87 (dd, $J_{6aA–5A} = 2.3$, $J_{6aA–6bA} = 12.2$ H-6bA); 3.89 (m, H-2B); 4.01 (dd, $J_{6bB–6aB} = 12.4$, $J_{6bB–5B} = 7.5$, H-6bB); 4.09 (m, H-5B); 4.11 (t, $J_{3A–2A} = 5.4$, $J_{3A–4A} = 5.4$ H-3B); 4.31 (s, H1-B); 5.25 (d, $J_{1A–2A} = 3.9$, H-1A). ^{13}C NMR (D_2O): 62.1 (C-6aB, C-6bB); 63.2 (C-6aA, C-6bA); 71.7 (C-2B); 71.8 (C1-B); 71.9 (C3-B); 72.1 (C4-A); 74.0 (C-2A); 75.4–76.6 (C-3A, C-5A, C-4B), 79.4 (C-5A).

4.3.8. 1α-(β′-Maltosyl)-1,5-anhydro-maltitol 16. Compound **14** (570 mg, 0.226 mmol) was deprotected as described for compound **4** obtaining **16** in quantitative yield. MALDI-MS: $m/z = 673$ [M+Na^+], 689 [M+K^+]. ^{1}H NMR (D_2O, four rings are termed for convenience: AB–CD) 3.39 (dd, H-4D); 3.41 (dd, H-4A); 3.52 (ddd, $J_{5C–6aC} = 5.0$, $J_{5C–6bC} = 2.0$, $J_{5C–4C} = 9.5$, H-5C); 3.54 (dd, $J_{2A–1A} = 3.9$, $J_{2A–3A} = 6.5$, H-2A); 3.56 (dd, $J_{2D–1D} = 3.9$, $J_{2D–3D} = 6.5$, H-2D); 3.59 (t, $J_{4B–3B} = 7.0$, $J_{4B–5B} = 7.0$, H-4B); 3.64 (t, $J_{4C–3C} = 8.5$, $J_{4C–5C} = 8.5$, H-4C); 3.65–3.72 (m, H-3A, H-5A, H3D, H-5D); 3.66 (m, H-1C); 3.68 (m, H-2C); 3.70 (m, H-3C); 3.73–3.78 (m, H-6aA, H-6aB, H-6aD); 3.77 (m, H-6aC); 3.81–3.74 (m, H-6bA, H-6bB, H-6bD); 3.90 (dd, $J_{2B–1B} = 5.3$, $J_{2B–3B} = 7.3$, H-2B); 3.91 (dd, $J_{6bC–5C} = 2.3$, $J_{6bC–6aC} = 13.2$, H-6bC); 4.03 (ddd, $J_{5B–} = 3.4$, $J_{5B–} = 6.4$, $J_{5B–} = 10.2$, H-5B); 4.27 (dd, $J_{1B–2B} = 5.3$, $J_{1B–1C} = 2.5$, H-1B); 4.31 (t, $J_{3B–2B} = 7.1$, $J_{3B–4B} = 7.1$, H-3B); 5.28 (d, $J_{1D–2D} = 3.9$, H-1D); 5.39 (d, $J_{1A–2A} = 3.9$, H-1A). ^{13}C NMR (D_2O): 63.0–63.2 (C-6aA, C-6bA, C-6aB, C-6bB, C-6aD, C-6bD); 63.7 (C-6C); 72.1–72.2 (C-4A, C-4D); 73.2 (C-2B); 73.9 (C-1B); 74.3–74.5 (C-2A, C-2D); 74.5 (C-2C); 74.6 (C-3B); 75.4–75.6 (C-3A, C-5A, C-3D, C-5D); 78.2 (C-5B); 78.8 (C-4B); 79.3 (C-4C); 80.8 (C-3C); 81.0 (C-5C); 83.9 (C-1C); 101.3 (C-1D); 102.3 (C-1A).

4.4. Conformation analysis methods

All the calculations were carried out using MACROMODEL 7.1 version of BATCHMIN on a SGO2 workstation. The force field used for energy minimization was AMBER* which includes Homan's parameters for pyranose.[11] The GB/SA (generalized Born/surface area) continuum water solvation model was used.[12] 1D-Ramachandran plots were calculated increasing θ angle from 0° to 360° by 1° increments. MC/EM simulations were performed on **16**, **11** and **5** using 30,000, 80,000 and 100,000 steps, respectively.

Acknowledgements

Dott. A. Naggi and Dott. G. Torri, for discussion and Dott. Elena Urso for Mass Spectra, Istituto 'G. Ronzoni'. Prof. J.-M. Savéant, for discussion and Prof. M. Robert for discussion and cyclic voltammetry, Laboratoire d'electrochimie organique, CNRS, Paris 7, France. This work was partially supported by EU (contract number QLK3-CT-2002-02049) and by Italian Ministry of research FIRB project (contract number RBAU01LF3E).

References

1. Levy, D. E.; Tang, C. In *The Chemistry of C-Glycosides*; Baldwin, J. E., Magnus, P. D.; Eds., Tetrahedron Organic Chemistry Series, Pergamon, Vol. 13, 1995.
2. Petitou, M.; Herault, J.-P.; Lormeau, J.-C.; Helmboldt, A.; Mallet, J.-M.; Sinay, P.; Herbert, J.-M. *Bioorg. Med. Chem.* **1998**, *6*, 1509–1516.
3. Alberti, A.; Della Bona, M.; Macciantelli, D.; Pelizzoni, F.; Sello, G.; Torri, G.; Vismara, E. *Tetrahedron* **1996**, *52*, 10241–10248.
4. Guerrini, M.; Mussini, P. M.; Rondinini, S.; Torri, G.; Vismara, E. *J. Chem. Soc., Chem. Commun.* **1998**, 1575–1576.
5. Rondinini, S.; Mussini, P. M.; Sello, G.; Vismara, E. J. *Electrochem. Soc.* **1998**, *145*, 1108–1112.
6. (a) Ref. 1, page 15 and references cited therein; (b) Drickamer, K. Molecular Structure of Animal Lectins. In *Molecular Biology*; Fukuda, M., Hindsgaul, O., Eds.; Oxford University Press: Oxford, 1994; p 65.
7. (a) Capila, I.; Linhardt, R. J. *Angew. Chem., Int. Ed.* **2002**, *41*, 390–412; (b) Parish, C. R.; Freeman, C.; Brown, K. J.; Francis, D. J.; Cowden, W. B. *Cancer Res.* **1999**, *59*, 3433–3441.
8. Vismara, E., unpublished results.
9. Kochi, J. K.; Rust, F. F. *J. Am. Chem. Soc.* **1961**, *83*, 2017–2018.
10. Naidoo, K. J.; Kuttel, M. J. *Comput. Chem.* **2000**, *22*, 445–456.
11. Homans, S. W. *Biochemistry* **1990**, *29*, 9110–9118.
12. Still, W. C.; Tempczyk, A.; Hawley, R.; Hendrickson, T. J. *Am. Chem. Soc.* **1990**, *112*, 6127–6129.